Available online at www.sciencedirect.com

SCIENCE DIRECT®

Tetrahedron: Asymmetry

Tetrahedron: *Asymmetry* 17 (2006) 975–983

NMR studies of chiral recognition mechanisms: interaction of enantiomers of *N*-imidazole derivatives with cyclodextrin hosts. Correlation with the CD-EKC studies

Cécile Danel,[a] Nathalie Azaroual,[b] Catherine Foulon,[a] Jean-François Goossens,[a] Gaston Vermeersch,[b] Jean-Paul Bonte[a] and Claude Vaccher[a,*]

[a]*Laboratoire de Chimie Analytique, EA 4034, Faculté des Sciences Pharmaceutiques et Biologiques, Université de Lille 2, 3 rue du Pr. Laguesse, BP 83, 59006 Lille Cédex, France*

[b]*Laboratoire de Physique, UMR CNRS 8009, Faculté des Sciences Pharmaceutiques et Biologiques, Université de Lille 2, BP 83, 59006 Lille Cédex, France*

Received 8 February 2006; accepted 23 March 2006

Abstract—The inclusion complexes formed between two chiral *N*-imidazole derivatives and four cyclodextrins (α-, β-, γ-, and highly sulfated-β-CDs) were investigated by one- and two-dimensional ^{1}H NMR. With the additional results of an ESI-MS study, a 1:1 stoichiometry was proven for all the complexes studied. The complexes were also characterized in terms of binding constants and the results were compared to those obtained by CD-EKC. An identical affinity order for the various CDs was obtained with both techniques. Furthermore, the affinity order for both enantiomers determined by their binding constants values is confirmed by the enantiomer migration orders previously determined by CD-EKC. The structural data obtained by the 2D-ROESY experiments allowed us to understand the interaction mechanisms and to propose, for different analyte structures, theoretical models of inclusion orientation in the CD cavity. These models are in accordance with our previous hypothesis based on the analyte structure–enantioseparation relationships and the thermodynamic parameters determined by CD-EKC.

1. Introduction

In the intermolecular interactions of host–guest type, cyclodextrins, due to their ability to form inclusion complexes with a great variety of molecules, seem to be the most interesting hosts. Their pharmaceutical applications rely on their capacity to enhance the solubility, stability, and bioavailability of drug molecules.[1] Furthermore, CDs are widely used as chiral selectors for the enantioresolution of drugs in separation techniques as high-performance liquid chromatography (HPLC)[2] or capillary electrophoresis (CE).[3] Electrokinetic chromatography using either neutral CDs or anionic CDs (CD-EKC) was previously performed to resolve the enantiomers of 10 new substituted [1-(imidazo-1-yl)-1-phenylmethyl]benzothiazolinone and benzoxazolinone derivatives.[4,5] These compounds, potential aromatase inhibitors, have been developed[6] according to the fadrozole, which is useful in second line therapy of estrogen dependent breast cancer in postmenopausal women.[7]

The formation of complexes between a ligand and a cyclodextrin is generally described as a result of inclusion of an apolar part of the ligand by hydrophobic interactions in the CD cavity and polar interactions between appropriate substituents of the ligand and the polar rim of the CD. However, the exact nature of the enantiomer discriminating interaction is still unclear and it is not possible to predict, which CD derivative is able to separate, which racemate.[3] The previous CD-EKC analyses have permitted us to obtain data about the mechanism of chiral recognition from the relations between analyte structure and electrophoretic behavior and from the determination of the binding constants and thermodynamic parameters.[4,5] Unfortunately, these data are averaged over the whole molecule and no structural information was obtained. An NMR spectroscopy study was achieved and this, by the

* Corresponding author. E-mail: claude.vaccher@univ-lille2.fr

0957-4166/$ - see front matter © 2006 Elsevier Ltd. All rights reserved.
doi:10.1016/j.tetasy.2006.03.019

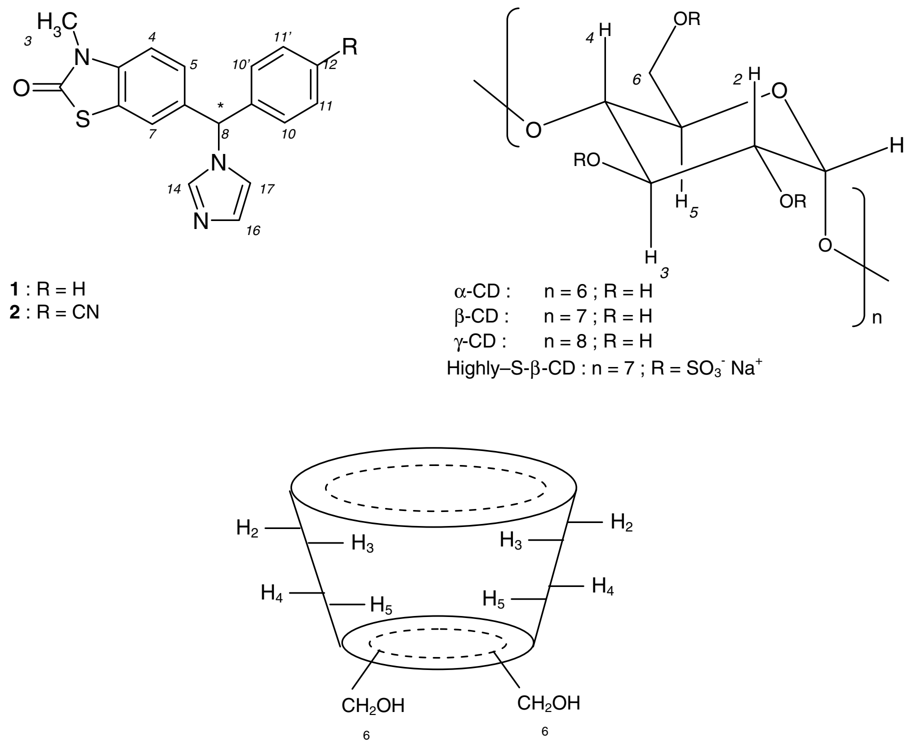

Figure 1. Structures and assignments of the hydrogen atoms of the aromatase inhibitors and the CDs.

complexation-induced chemical shifts of both the ligand and the CD, allowed us to obtain more valuable information on the complexes.[3,8] Chankvetadze et al. have published a series of papers to describe structural information of ligand–CDs complexes in CE solutions using NMR, electrospray ionization mass spectrometry (ESI-MS) and other spectroscopic techniques.[9–14] The chiral recognition of azole derivatives with cyclodextrin hosts have already been studied by Zhou et al.[15] (a triazole derivative with the γ-CD) and Endresz et al.[16] (the metomidate, imidazole derivative, with various neutral and anionic CDs).

Herein, to complete our previous CE studies, the intermolecular complexes formed between analytes **1** and **2** (Fig. 1) and CDs (α-, β-, γ-, and highly sulfated-β-CDs) were investigated by one-dimensional NMR study to determine the stoichiometry and the apparent binding constants, by a two-dimensional NMR study to provide structural informations through the observation of the intermolecular NOE effects. Furthermore, the stoichiometry was also studied by ESI-MS, which permits us to study the noncovalent interactions thanks to its soft ionization. It was possible to discriminate between 1:1 and 2:2 complexes.[8] Herein, the complete study is developed for **1** whereas for **2** only the structural study is presented.

2. Results and discussion

2.1. Stoichiometry determination

The stoichiometry of the complexes formed between **1** and the α-, β-, γ-, or highly S-β-CDs (n:m complexes) was first determined by ^{1}H NMR spectra by measurement of the variations in the chemical shifts of both the analyte and CD induced by complexation using the continuous variation method developed by Job.[17] According to the ^{1}H NMR spectra obtained for the various molar ratios r, only some hydrogen atoms of the analyte and the CDs can be selected for the measurement of their chemical shifts. For example, the signal H_{14} of **1** allowed us to obtain Job's plots for the four complexes studied. The continuous variation plots, showing a maximum for a molar ratio of 0.5, indicate that a favorable stoichiometric ratio of n:n occurs for the various CDs (Fig. 2). Similar curve shapes with a maximum value for $r = 0.5$ were obtained for all the studied signals of **1** (H_3, H_8, H_{14}, H_{16}) with all CDs. In the case

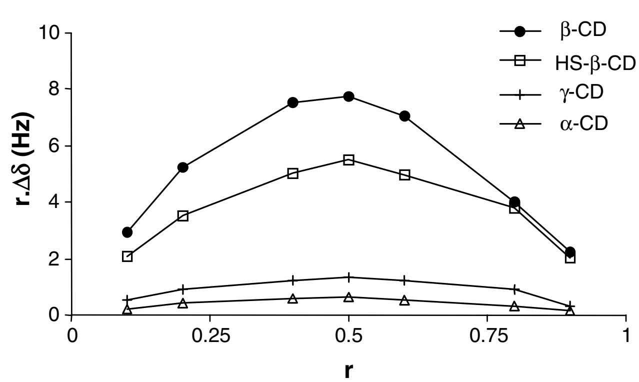

Figure 2. Job's plots for the protons H_{14} in the (R)-**1**·α-CD, (R)-**1**·β-CD, (R)-**1**·γ-CD, and (R)-**1**·highly S-β-CD complexes ($r = [(R)\text{-}\mathbf{1}]/([(R)\text{-}\mathbf{1}] + [\text{CD}])$).

of the (*R*)-**1**·β-CD complex, it is worth mentioning that the H_1 and H_4 signals of the β-CD displayed smaller chemical shift differences than the H_3 signal (Fig. 3). Since the H_3 hydrogen is located into the cavity, this is consistent with an inclusion of an analyte part in the CD cavity. Same results were observed for the *n*:*n* (*S*)-**1**·CDs complex.

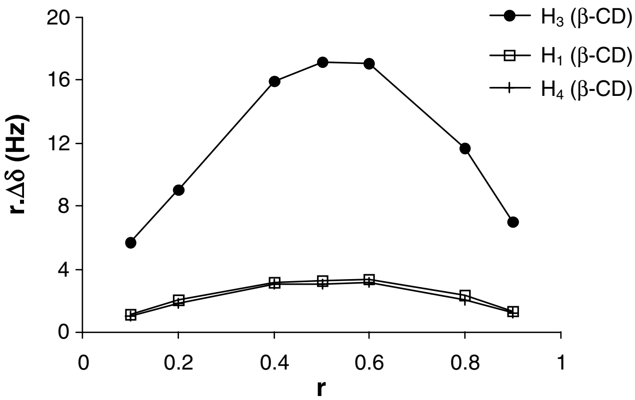

Figure 3. Job's plots for the protons H_1, H_3, and H_4 of β-CD in the (*R*)-**1**·β-CD complex ($r = [(R)\text{-}\mathbf{1}]/([(R)\text{-}\mathbf{1}] + [\text{CD}])$).

The complexes were then studied by ESI-MS; the spectra obtained are presented in Figure 4. The lowest remarkable *m*/*z* ratios correspond to (*rac*)-**1** and its dimeric form; higher *m*/*z* ratios were observed for the various CDs and their ammonium adducts and the highest *m*/*z* ratios detected at 1295, 1457, and 1619 correspond to the **1**·α-CD-H^+, **1**·β-CD-H^+, and **1**·γ-CD-H^+ complexes, respectively. The absence of any signal for higher *m*/*z* ratios confirms the *n*:*n* stoichiometry previously determined by ^{1}H NMR and permits especially to attribute the 1:1 stoichiometry ($n = 1$). Unfortunately, it was not possible to study by ESI-MS the complex formed with the highly S-β-CD, since these CDs are marketed as an heterogeneous mixture and its ESI-MS spectrum presents too many peaks.

In the CD-EKC studies, the 1:1 stoichiometry of the complexes was already supposed, since the Wren and Rowe model[18] was verified and have permitted to determine the binding constants of the complexes.

2.2. Apparent binding constants determination

For the complexes of known 1:1 stoichiometry, the Scott's modification[19] of the Benesi–Hildebrand method[20] was used to calculate the apparent binding constants according to Eq. 1:

$$\frac{[\text{CD}]}{\Delta\delta} = \frac{[\text{CD}]}{\Delta\delta_c} + \frac{1}{K\Delta\delta_c} \qquad (1)$$

[CD] is the equilibrium molar concentration of the CD (equal to the total introduced CD concentration since it is present in large excess in comparison with the analyte concentration); $\Delta\delta$ is the observed chemical shift difference for a given [CD]; $\Delta\delta_c$ is the chemical shift difference between a pure sample of the complex at the saturation and the free component. The determination of the slope and the intercept with the *y*-axis of the plot $[\text{CD}]/\Delta\delta$ against [CD] allows an estimation of the apparent binding constant. According to this model, the apparent binding constants were determined for the eight complexes formed between each enantiomer of **1** and the α-, β-, γ-, or highly S-β-CDs. The effect of the addition of great amounts of CD on the aromatic part of the analyte is illustrated in the case of the (*R*)-**1**·β-CD complex (Fig. 5). The chemical shifts of some signals can be seen (as H_8, H_{10}, H_{14}, and H_{16}, since other signals are not well resolved). Table 1 summarizes the chemical shift differences observed for the H_{14} signal with addition of α-, β-, γ-, and highly S-β-CDs. Linear Scott's plots were obtained for the eight complexes, the r^2

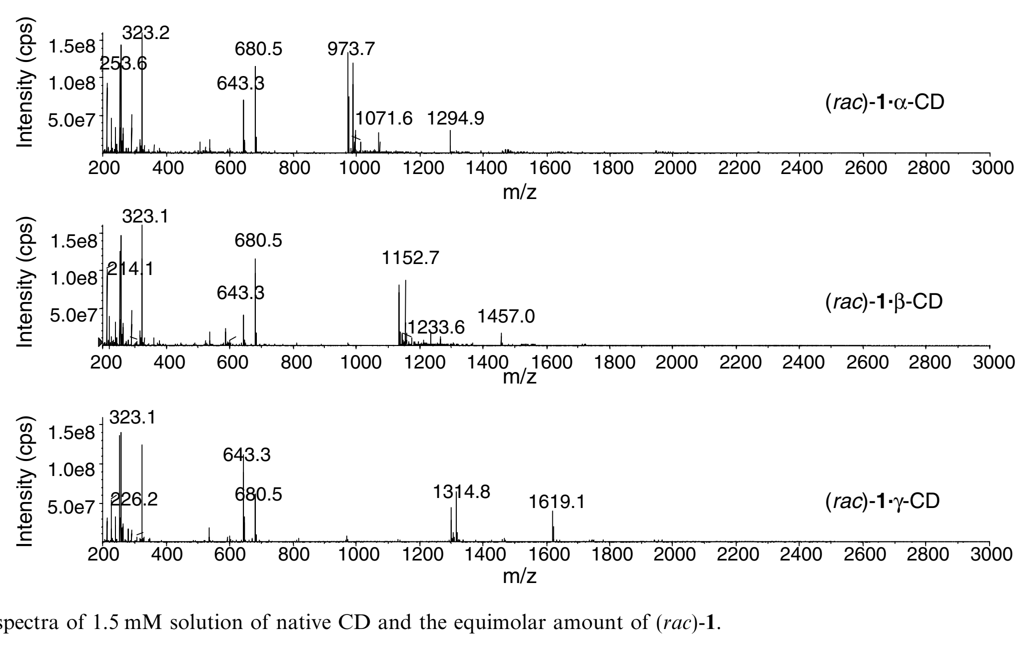

Figure 4. ESI-MS spectra of 1.5 mM solution of native CD and the equimolar amount of (*rac*)-**1**.

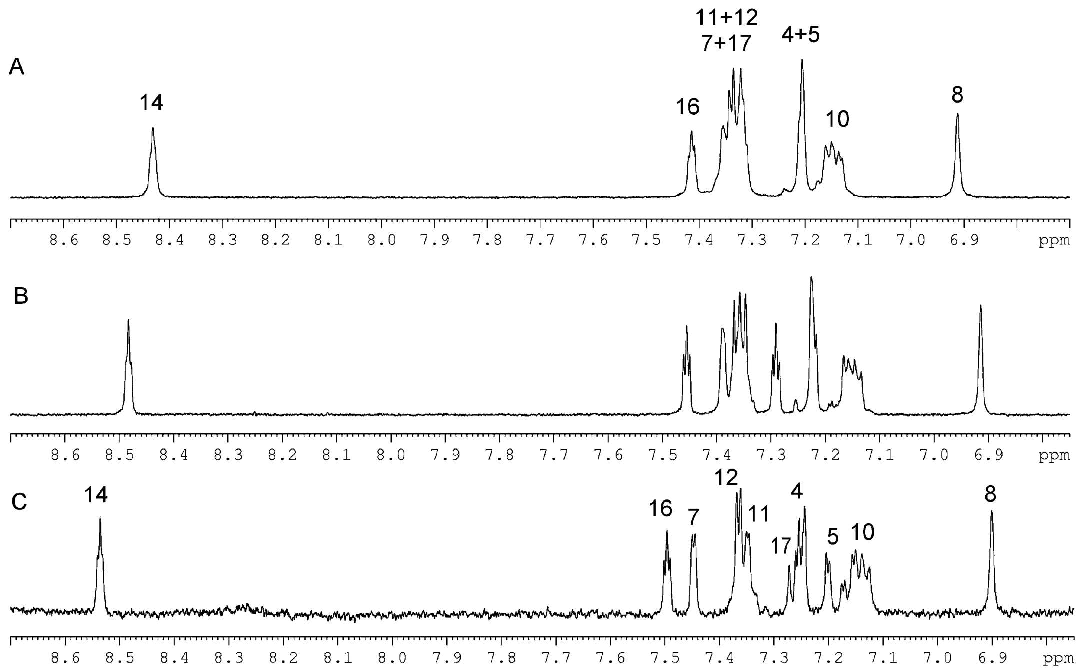

Figure 5. Aromatic part of the ^{1}H NMR spectra of (R)-**1** without CD (A) and after addition of 8 (B) and 24 (C) equiv of β-CD.

Table 1. Chemical shift difference ($\Delta\delta$) observed for the H_{14} signal of (R)-**1** with addition of α-, β-, γ-, and highly S-β-CDs

(R)-**1**·α-CD Complex						
[α-CD]/[(R)-**1**]	6.8	10.2	13.6	20.4	27.2	
$\Delta\delta$ (Hz)	2.7	3.3	3.8	4.9	5.7	
(R)-**1**·β-CD Complex						
[β-CD]/[(R)-**1**]	8	12	16	18	20	24
$\Delta\delta$ (Hz)	14.6	19.5	23.5	24.9	26.4	29.1
(R)-**1**·γ-CD Complex						
[γ-CD]/[(R)-**1**]	10	15	20	25	30	40
$\Delta\delta$ (Hz)	6.5	8.9	11.3	12.9	14.5	17.8
(R)-**1**·Highly S-β-CD complex						
[HS-β-CD]/[(R)-**1**]	10	15	20	25	30	40
$\Delta\delta$ (Hz)	41.3	42.5	43.1	44.0	45.0	46.8

values for the linear fit were greater than 0.90. The apparent and averaged binding constants of the complexes formed between either (R)-**1** or (S)-**1** and the four CDs, are reported in Table 2. It appears that some quantitative differences do exist between the binding constants calculated on the basis of different ^{1}H NMR signals. However, an identical rank can be proposed whatever the signal studied. The lowest apparent and averaged binding constants were obtained with the α- and γ-CDs. The β-CD permits higher complexations but lower than those obtained with the anionic highly S-β-CD. It seems that the β-CD cavity size adjusts to permit the fit of the analyte in the cavity whereas the α- and γ-CDs cavity size must be either too small or too large to favor the inclusion and inclusion maintenance, respectively. The apparent binding constants for the **1**·highly S-β-CD complexes appear to be greater than those obtained with native CDs [e.g., taking into account the H_{14} signal, K are 215 and 429 M^{-1} for (R)-**1**·β-CD and (R)-**1**·highly S-β-CD, respectively]. When the highly S-β-CD

Table 2. Apparent and averaged binding constants (K in M^{-1}) determined by ^{1}H NMR or CD-EKC[4,5] for the complexes formed between **1** and various CDs [for the ^{1}H NMR study, K is calculated on the basis of the H_{16}, H_{14}, H_{10}, or H_8 signals of (R)-**1** or (S)-**1**]

	^{1}H NMR study			CD-EKC study[a]
	K (H_{16})	K (H_{14})	K (H_8)	
(R)-**1**·α-CD	n.d.	60	15	49
(S)-**1**·α-CD	n.d.	<10	<10	49
(R)-**1**·β-CD	242	215	241	322
(S)-**1**·β-CD	157	154	185	281
(R)-**1**·γ-CD	25	17	25	25
(S)-**1**·γ-CD	20	18	20	25
(R)-**1**·Highly S-β-CD	268	429	394	2835
(S)-**1**·Highly S-β-CD	211	330	225	2835

n.d.: K cannot be determined with this signal.
The errors associated with these experiments are under 10% and 5% for the ^{1}H NMR and CD-EKC studies,[4,5] respectively, and make the K differences obtained for both enantiomers significant in all cases.
[a] Mean values calculated from three experiments.

and analyte have opposite charges, the interaction seems to be strengthened by ion-pairing or an electrostatic mechanism.

Due to the use of similar experimental conditions in ^{1}H NMR and CD-EKC (except the addition of 15% methanol in the phosphate buffer necessary to the solubilization of the analyte for NMR solutions), the apparent binding constants determined by NMR and CD-EKC can be compared. The constants determined by CD-EKC for the complexes formed between (*R*)-**1** and α, β-, γ-, or highly S-β-CDs are 49, 322, 25, or 2835 M^{-1}, respectively, and for the complexes formed between (*S*)-**1** and α, β-, γ-, or highly S-β-CDs, 49, 281, 25, or 2835 M^{-1}, respectively (enantiomers of **1** are only resolved by the β-CD). Comparison of the results shows that the constants are greater in CD-EKC than in ^{1}H NMR: this could be partly due to the presence of methanol, which induces a competition with the analyte for the CD cavities. Furthermore, the differences may result from different principles of measurement in NMR and CD-EKC. However, an identical affinity order for the various CDs was obtained with both techniques [K (**1**·γ-CD) < K (**1**·α-CD) < K (**1**·β-CD) < K (**1**·highly S-β-CD)]. Concerning the apparent binding constants determined by NMR for both enantiomers, the results are in accordance with the enantiomer migration orders previously determined by CD-EKC when enantioseparations occurred: (*R*)-**1** appears to be the most complexed enantiomer in all cases.

2.3. Structure of the complexes

The interactions between the enantiomers of **1** and the α-, β-, γ-, or highly S-β-CDs were investigated in more detail by two-dimensional rotating frame Overhauser effect spectroscopy (2D-ROESY) since this technique allows us to obtain reliable data on the structure of guest–CD complexes.[21]

2.3.1. Analyte·native CD complexes. When α- and γ-CD were used, the dipolar correlations were too weak to be detected by ^{1}H NMR. This result is consistent with the weak apparent binding constants determined for the **1**·α-CD and **1**·γ-CD complexes.

The partial 2D-ROESY spectrum of the (*R*)**1**·β-CD is reported in Figure 6. First, an intramolecular (*R*)-**1** interaction between H_4, H_5, and the H_3 bearing by the methyl group is detected. Secondly, intermolecular interactions were observed between various protons of the analyte and the H_3 and/or H_6 of the β-CD, these three protons being not resolved. To attribute these cross-peaks to H_3 or H_6, a 1D-ROESY experiment was performed by irradiating the well resolved proton H_8 of (*R*)-**1** and observing the response on the various protons of the β-CD: the NOE response was observed only for the H_3 of the β-CD by the presence of a triplet (Fig. 7). The cross-peaks observed for the various protons of the phenyl group (H_{10}, H_{11}, and/or H_{12}) were then attributed to the H_3 of the β-CD. Furthermore, the inspection of this map allows us to establish spatial proximity between these aromatic protons and the H_5 of the β-CD: it is worth mentioning that the interactions observed for the H_{11} and/or H_{12} are greater than the one observed for H_{10}. The H_3 and H_5 being located inside the CD cavity (with H_3 nearer to the secondary rim), these results show that the complexation occurs through the inclusion of the phenyl moiety into the hydrophobic cavity of the β-CD in an axial orientation and that the molecule enters the cavity very deeply from the secondary rim.

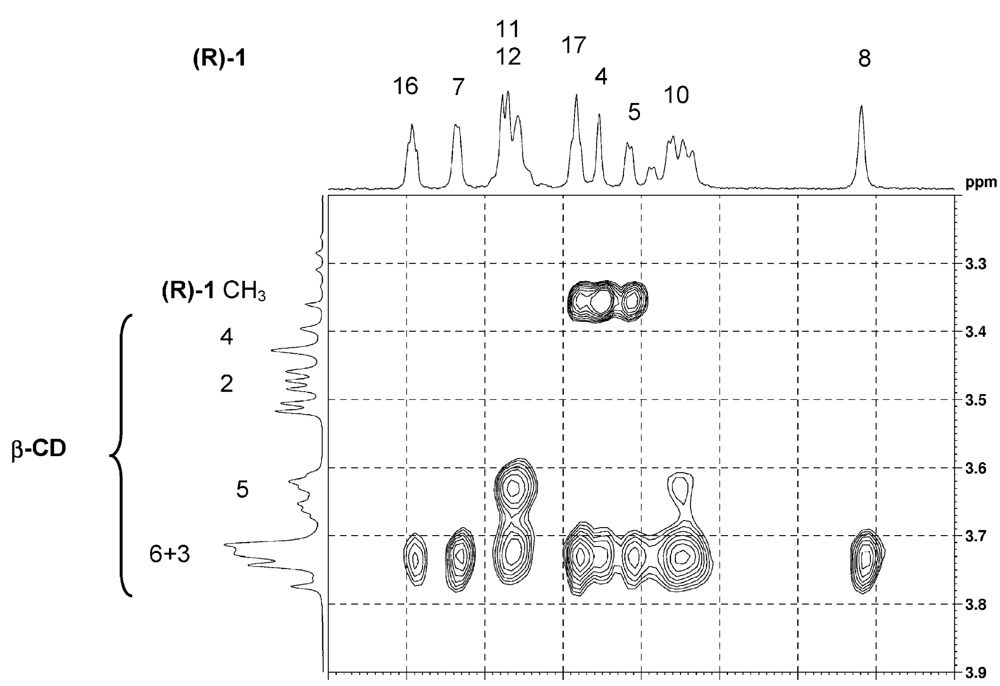

Figure 6. Partial ROESY spectrum of the (*R*)-**1**·β-CD complex ([**1**] = 1 mM, [β-CD] = 4 mM).

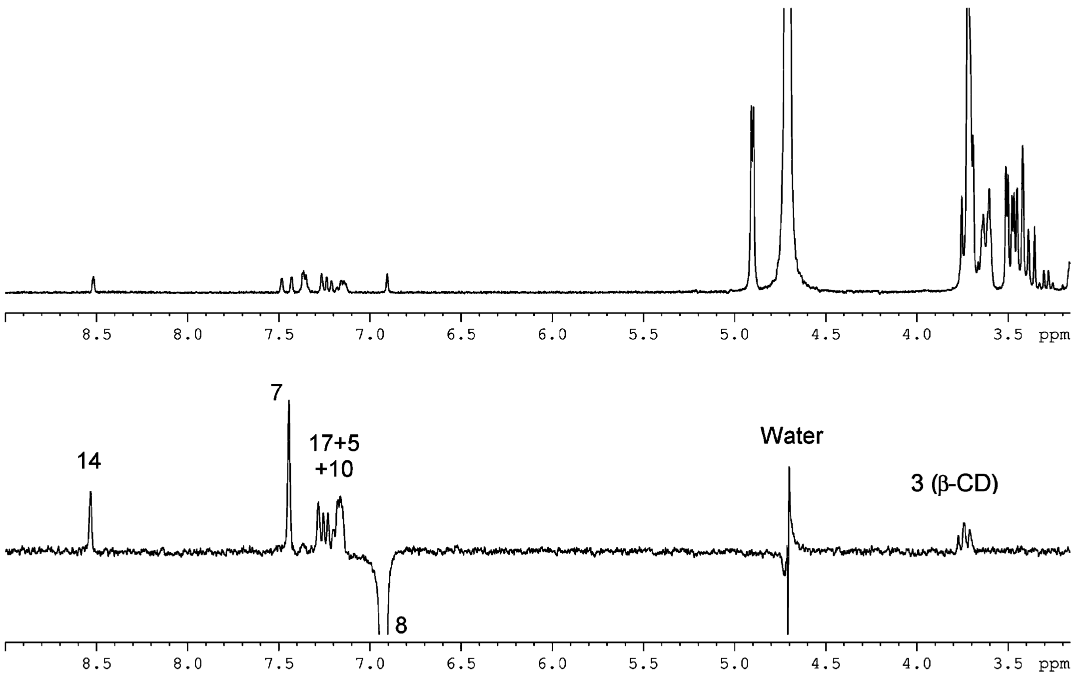

Figure 7. ^{1}H NMR spectrum of the (*R*)-**1** and ^{1}H NMR ROESY spectrum with irradiation of H_8, in presence of 4 equiv of β-CD.

The phenyl ring of the analyte having an important role in the complexation mechanism, the structure of the complex formed between (*R*)-**2** and the β-CD was studied [**2** being the analogue of **1** with a *para*-cyano substitution on the phenyl ring]. The presence of the cyano group instead of the H_{12} leads to two major modifications of the 2D-ROESY spectrum (Fig. 8). Firstly, no cross-peak was detected for H_{16}. Secondly, the correlation with H_{17}, which was one of the most intense for the (*R*)-**1**·β-CD complex, has disappeared for the (*R*)-**2**·β-CD complex. These results suggest the importance of the *para*-cyano substitution of the phenyl ring on the inclusion complexation and lead us to propose two complexation models for the (*R*)-**1**·β-CD and (*R*)-**2**·β-CD complexes (Fig. 9). This proposition was in accordance with the previous CD-EKC results.[4]

2.3.2. Analyte·highly S-β-CD complexes. To observe the effect of the sulfate substitution of the β-CD on the analyte complexation, the (*R*)-**1**·highly S-β-CD and (*R*)-**2**·highly S-β-CD complexes were also studied. The 2D-ROESY

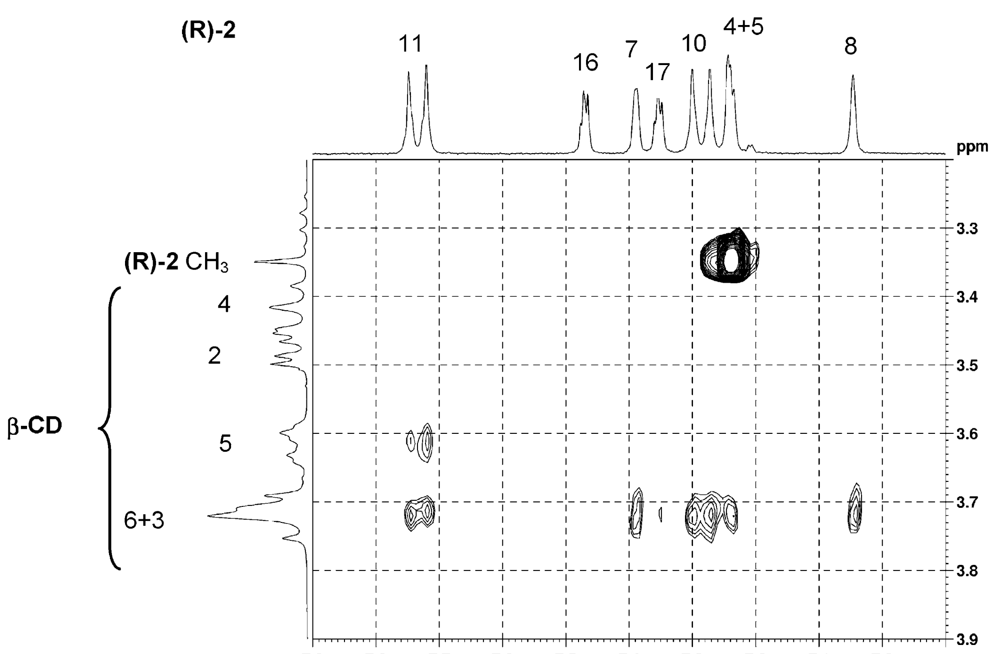

Figure 8. Partial ROESY spectrum of the (*R*)-**2**·β-CD complex ([**2**] = 2 mM, [β-CD] = 2 mM).

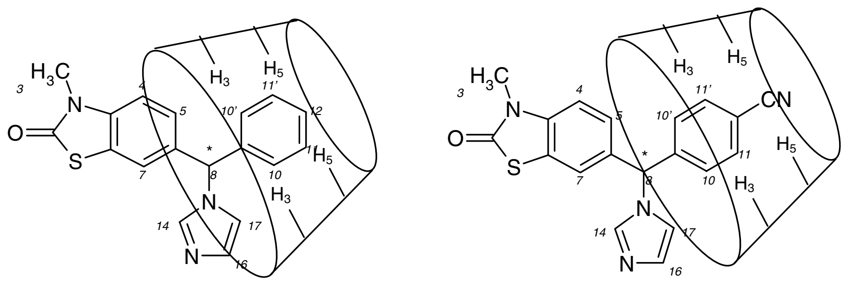

Figure 9. Proposed models for the inclusion of (*R*)-**1** and (*R*)-**2** in the β-CD.

map obtained for the (*R*)-**1**·highly S-β-CD complex is reported in Figure 10: in addition to the intramolecular interactions between the H_3 and H_4, H_5 of the analyte, most important cross-peaks were observed between the H_3 and/or H_5 of the highly S-β-CD and the H_{10}, H_{11}. However, the absence of cross-peaks for the H_{12} was noted. These results suggest, once again that an inclusion of the phenyl ring in the CD cavity might occur but it might be different that the one observed with the native β-CD. The different orientation of the solute into the cavity may be correlated to the presence of electrostatic interactions between the cationic imidazol ring (at pH 2.5) and the negatively charged sulfate group on the CD rim. The influence of the *para*-cyano substitution of the analyte on the complexation was also studied with the (*R*)-**2**·highly S-β-CD complex. Although dipolar interactions were observed between the H_3 and/or H_5 of the highly S-β-CD and the H_{11} of the analyte, no cross-peak was observed for H_{10}. These results suggest an inclusion of the phenyl group in the CD cavity but less deep than the one considered for the (*R*)-**1**·highly S-β-CD complex. Identical 2D-ROESY maps were obtained for both enantiomers whatever the complex studied.

3. Conclusion

The mechanism of enantiorecognition of **1** and **2** with β- and highly S-β-CDs was previously studied by CD-EKC:[4,5] firstly, the comparison of the electrophoretic parameters of **1** and **2** in the presence of β- and highly S-β-CDs allowed a correlation between a higher analyte–CD interaction and a greater hydrophobicity of the phenyl moiety of the analytes (**1** is more hydrophobic than **2**); secondly, the important hydrophobic binding contribution to the analyte–CD complexation has been proven by calculations of the enthalpic and entropic parameters. In the present NMR study, the different complexation-induced chemical shifts of the analytes or the native CDs were successfully used for determination of the stoichiometry and apparent binding constants of the analyte–CD complexes of each enantiomer. These results obtained by NMR are in accordance with the CD-EKC studies. The 2D-ROESY experiments have permitted us to obtain structural information on the complexes and to propose inclusion complexation models (the inclusion of the phenyl moiety (substituted or not by a cyano group) in the hydrophobic

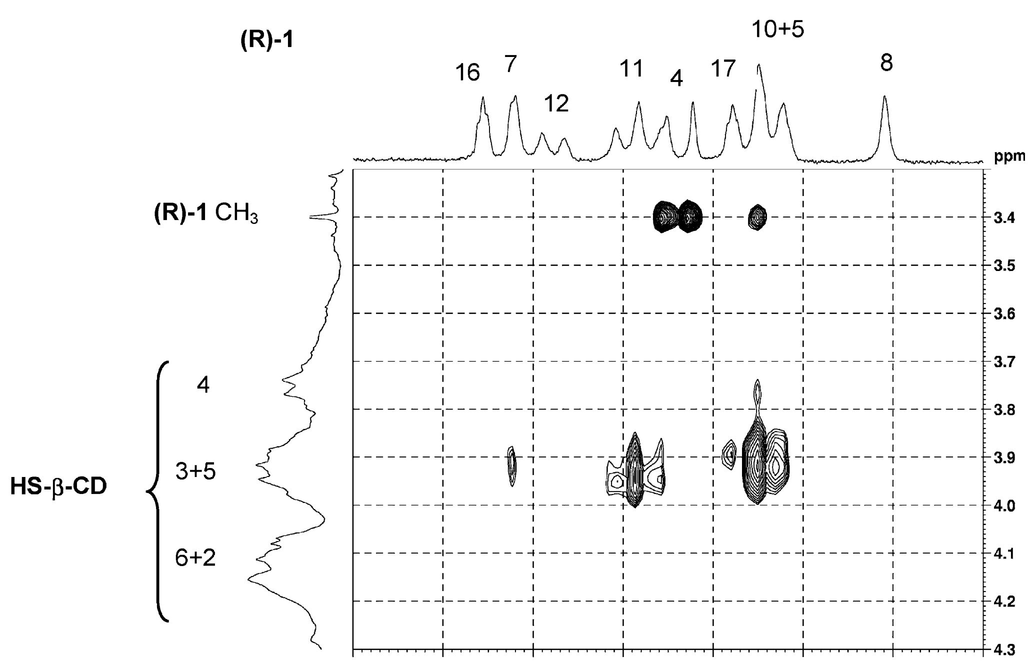

Figure 10. Partial ROESY spectrum of the (*R*)-**1**·highly S-β-CD complex.

cavities of these CDs). The understanding of the recognition mechanisms that occur with these chiral selectors was then improved by all these results.

4. Experimental

4.1. Chemicals

Analytes **1** and **2** were prepared according to the synthetic pathway previously described[6] leading to a racemic mixture. The enantiomers of **1** and **2** were obtained by preparative HPLC separation using polysaccharide chiral stationary phases; the absolute configuration (*R*) and (*S*) were attributed to the *dextro* (+) and *levo* (−) isomers, respectively.[22] α-CD and γ-CD were purchased from Wacker Chimie (Lyon, France) and Highly S-β-CD from Beckman (Beckman Coulter France, Villepinte, France). β-CD was a gift of the Roquette Laboratories (Lestrem, France). Deuterium oxide 100% and methyl-D_3-alcohol-D_1 were purchased from Euriso-top (Gif sur Yvette, France) and Aldrich (Lyon, France), respectively. Phosphoric acid (85% w/w) and triethylamine were purchased from Merck (Nogent-sur-Marne, France).

4.2. Nuclear magnetic resonance

All NMR experiments were carried out on a Bruker AVANCE 300 spectrometer operating at 300.09 MHz and equipped with a multinuclear *z*-gradient inverse probehead. Five hundred microliters of solutions were introduced into a standard 5 mm NMR tubes and the experiments were realized at 298 K.

One dimensional (1D) and two dimensional (2D) ROESY spectra were recorded with a mixing time of 500 ms during the spin-lock. Attributions of analyte proton resonances were realized by standard NMR experiments: COSY (correlation homonuclear ^1H–^1H), HSQC (correlation heteronuclear ^1H–^{13}C), HMBC (correlation long range ^1H–^{13}C).

4.2.1. Determination of the stoichiometry by the Job's plot. Both solutions of analyte (5 mM) and CDs (5 mM) were prepared in a 15/85 (% v/v) mixture of methanol and 100 mM D_2O phosphate buffer adjusting the pH to 2.5 with triethylamine (TEA). To obtain the desired ratio, which varied from 0 to 1, solutions were mixed while keeping the sum of both concentration constant (5 mM).

4.2.2. Determination of the apparent binding constant by the Scott's method. Solutions of both analyte and CDs were prepared in the same 15/85 (% v/v) solvent mixture. To be in accordance with the Scott's model and take into account that the equilibrium molar concentration of the CD is equal to the total introduced CD concentration, the concentration of the CD on the complexed form must be insignificant. The concentrations of the enantiomer were chosen lower as possible but sufficiently high to permit its NMR detection. In the NMR solutions, [(*R*)-**1**] and [(*S*)-**1**] were generally 1 mM except for the complexes formed with the β-CD (0.2 mM). The [analyte]/[CD] ratios were progressively increased from 6.8 to 27.2, 8 to 24, 10 to 40, and 10 to 40 for the α-, β-, γ-, and highly S-β-CDs, respectively.

4.2.3. Study of the structure of the complexes by 2D-ROESY experiments. To study the structure of the complexes by 2D-ROESY experiments, the choice of the concentrations of both analyte and CDs solutions prepared in the 15/85 (% v/v) solvent mixture results from a compromise between an high analyte concentration and a good separation of analyte resonance signals: for the **1**·α-CD, **1**·γ-CD and **2**·β-CD complexes, enantiomers and CDs are mixed in equivalent amount (2 mM), for the **1**·β-CD and **1**·highly S-β-CD complexes, [**1**] = 1 mM, [β-CD] = 4 mM and [highly S-β-CD] = 10 mM, for the **2**·highly S-β-CD, [**2**] = 1 mM and [highly S-β-CD] = 4 mM.

4.3. Electrospray ionization-mass spectrometry

Mass spectra were performed using a Applied Biosystems API 3000 instrument (PE Sciex, Toronto, Canada) equipped with an electrospray ion source. ESI-MS measurements were performed in positive mode with an ion spray voltage of 5000 V. Solutions of analytes **1** or **2** and α-, β-, or γ-CDs at 3 mM in water/methanol (95/5 %v/v) were mixed in an equivalent amount and 1% of formic acid was added to enhance the ionization. The samples were introduced into the ion source at a flow rate of 5 μL min^{-1}. Spectra were acquired by scanning *m*/*z* from 10 to 4000 with a 0.1 resolution.

Acknowledgments

The authors are grateful to Roquette Laboratories for the gift of β-CD and to Dr Kouach (Laboratoire de Spectrométrie de Masse, Faculté de Médecine, Lille, France) for helpful collaboration in the ESI-MS study. This work was supported by grants from the Ligue Nationale contre le cancer (Comité du Nord).

References

1. Hedges, A. R. *Chem. Rev.* **1998**, *98*, 2035–2044.
2. Subramanian, G. *A Practical Approach to Chiral Separations by Liquid Chromatography*; VCH: Weinheim, 1994.
3. Chankvetadze, B. *Capillary Electrophoresis in Chiral Analysis*; Wiley: Chichester, 1997.
4. Foulon, C.; Danel, C.; Vaccher, M. P.; Bonte, J. P.; Vaccher, C.; Goossens, J. F. *Electrophoresis* **2004**, *25*, 2735–2744.
5. Danel, C.; Lipka, E.; Bonte, J. P.; Goossens, J. F.; Vaccher, C.; Foulon, C. *Electrophoresis* **2005**, *26*, 3824–3832.
6. Nativelle-Serpentini, C.; Molesni, S.; Yous, S.; Park, C. H.; Lesieur, D.; Sourdaine, P.; Seralini, G. E. *J. Enzym. Inhib. Med. Chem.* **2004**, *19*, 119–127.
7. Njar, V. C. O.; Brodie, A. M. H. *Drugs* **1999**, *58*, 233–255.
8. Chankvetadze, B.; Blaschke, G. *Electrophoresis* **1999**, *20*, 2592–2604.
9. Chankvetadze, B.; Endresz, G.; Bergenthal, D.; Blaschke, G. *J. Chromatogr. A* **1995**, *717*, 245–253.
10. Chankvetadze, B.; Endresz, G.; Schulte, G.; Bergenthal, D.; Blaschke, G. *J. Chromatogr. A* **1996**, *732*, 143–150.
11. Chankvetadze, B.; Schulte, G.; Bergenthal, D.; Blaschke, G. *J. Chromatogr. A* **1998**, *798*, 315–323.

12. Chankvetadze, B.; Pintore, G.; Burjanadze, N.; Bergenthal, D.; Strickmann, D.; Cerri, R.; Blaschke, G. *Electrophoresis* **1998**, *19*, 2101–2108.
13. Chankvetadze, B.; Pintore, G.; Burjanadze, N.; Bergenthal, D.; Bergander, K.; Breitkreuz, J.; Mühlenbrock, C.; Blaschke, G. *J. Chromatogr. A* **2000**, *875*, 455–469.
14. Chankvetadze, B.; Burjanadze, N.; Pintore, G.; Bergenthal, D.; Bergander, K.; Mühlenbrock, C.; Breitkreuz, J.; Blaschke, G. *J. Chromatogr. A* **2000**, *875*, 471–484.
15. Zhou, L.; Thompson, R.; Reamer, R. A.; Miller, C.; Welch, C.; Ellison, D. K.; Wyvratt, J. M. *J. Chromatogr. A* **2003**, *987*, 409–420.
16. Endresz, G.; Chankvetadze, B.; Bergenthal, D.; Blaschke, G. *J. Chromatogr. A* **1996**, *732*, 133.
17. Job, P. *Ann. Chim.* **1928**, *9*, 113–203.
18. Wren, S. A. C.; Rowe, R. C. *J. Chromatogr.* **1992**, *603*, 235–241.
19. Scott, R. L. *Recl. Trav. Chim.* **1956**, *75*, 787–789.
20. Benesi, H. A.; Hildebrand, J. H. *J. Am. Chem. Soc.* **1949**, *71*, 2703–2707.
21. Schneider, H. J.; Hacket, F.; Rüdiger, V.; Ikeda, H. *Chem. Rev.* **1998**, *98*, 1755–1785.
22. Danel, C.; Foulon, C.; Guelzim, A.; Park, C. H.; Bonte, J. P.; Vaccher, C. *Chirality* **2005**, *17*, 600–607.